Published OnlineFirst July 18, 2013; DOI: 10.1158/0008-5472.CAN-13-0545

Cancer Research

Tumor Microenvironmental Conversion of Natural Killer Cells into Myeloid-Derived Suppressor Cells

Young-Jun Park, Boyeong Song, Yun-Sun Kim, et al.

Cancer Res 2013;73:5669-5681. Published OnlineFirst July 18, 2013.

Published OnlineFirst July 18, 2013; DOI: 10.1158/0008-5472.CAN-13-0545

Tumor Microenvironmental Conversion of Natural Killer Cells into Myeloid-Derived Suppressor Cells

Young-Jun Park[1], Boyeong Song[2], Yun-Sun Kim[1], Eun-Kyung Kim[1], Jung-Mi Lee[1], Ga-Eun Lee[1], Jae-Ouk Kim[3], Yeon-Jeong Kim[4], Woo-Sung Chang[1], and Chang-Yuil Kang[1,2]

Abstract

How myeloid-derived suppressor cells (MDSC) emerge in the tumor environment remains unclear. Here, we report that GM-CSF can convert natural killer (NK) cells into MDSCs. When transferred into tumor-bearing mice, adoptively transferred NK cells lost their NK phenotype and were converted into $Ly6C^{high}Ly6G^{high}$ MDSC. This conversion was abolished by exposure to IL-2 either *in vitro* or *in vivo*. Notably, we found that of the 4 maturation stages based on CD11b/CD27 expression levels, only the $CD11b^{high}CD27^{high}$ NK cells could be converted into $CD11b^{+}Gr1^{+}$ MDSC *ex vivo*. Transfer of $CD27^{high}$ NK cells from tumor-bearing mice into tumor-bearing recipients was associated with conversion to MDSC in a manner associated with reduced numbers of $CD11b^{high}CD27^{high}$ and $CD11b^{high}CD27^{low}$ NK cell populations in the recipients. Our results identify a pathway of MDSC development from immature NK cells in tumor-bearing hosts, providing new insights into how tumor cells modulate their host immune microenvironment to escape immune surveillance. *Cancer Res; 73(18); 5669–81. ©2013 AACR.*

Introduction

The tumor environment recruits diverse suppressor cells, such as M2 macrophages, regulatory T cells, and myeloid-derived suppressor cells (MDSC; refs. 1–3), to help cancer cells evade the attack by effector cells, leading to the subversion of the immune surveillance (3). Of the suppressor cells, MDSCs comprise a mixed population of immature myeloid cells that accumulate in various pathologic conditions, particularly in tumors. Recently, the morphologic heterogeneity of MDSCs has been classified by the expression of Ly6C and Ly6G molecules, which has led to the identification of 2 MDSC subsets, i.e., $CD11b^{+}Ly6G^{+}Ly6C^{low}$ polymorphonuclear (PMN)-MDSCs and $CD11b^{+}Ly6G^{-}Ly6C^{high}$ monocytic (Mo)-MDSCs (4). MDSCs use multiple mechanisms to suppress the adaptive and innate immune systems and increased numbers of MDSCs correlate with a poor prognosis in patients with cancer (5, 6). Recent studies have shown that a small number of transcription factors regulate aberrant myelopoiesis, leading to MDSC expansion (7–9). Despite the advances in the field, the MDSC developmental pathway remains in part elusive.

In contrast with MDSCs, natural killer (NK) cells present barriers to various tumors (10). NK cell depletion leads to enhanced tumor growth in a mouse tumor model, indicating clearly the involvement of NK cells in tumor surveillance (11). In addition, it has been shown that improved disease prognosis is associated with the extent of NK cell infiltration in non–small cell lung carcinomas and colorectal cancers (12). However, in a number of cases, NK cells in the tumor environment exhibit maturation and functional defects, decreasing the absolute number of cells (13–15). Although a number of studies are underway to determine the cause of NK cell abnormalities, further investigations will be required.

In this study, we describe the unprecedented phenomenon that conventional NK cells in a specific maturation state in the tumor environment are converted into MDSCs in tumor-bearing mice. The number of NK cells decreased significantly as the implanted tumor grows, which may be attributed to the conversion of $CD11b^{high}CD27^{high}$ NK cells into MDSCs rather than being matured into $CD11b^{high}CD27^{low}$ phenotype. NK cell-activating cytokine, interleukin (IL)-2, inhibited the development of MDSCs from NK cells *in vitro* and *in vivo*. Overall, *in vivo* IL-2 treatment induced NK cell expansion, augmented the activity of the cells, and may result in the regression of tumor growth.

Materials and Methods

Mice and cell lines

All experiments were approved by the Institutional Animal Care and Use Committee of Seoul National University (Seoul, Korea). Six-week-old BALB/c, C57BL/6 mice were purchased

Authors' Affiliations: [1]Laboratory of Immunology, Research Institute of Pharmaceutical Sciences, College of Pharmacy; [2]WCU, Department of Molecular Medicine and Biopharmaceutical Science, Graduate School of Convergence Science and Technology, Seoul National University; [3]Neonatal Vaccinology Section, International Vaccine Institute, SNU Research Park; and [4]Laboratory of Microbiology and Immunology, College of Pharmacy, Inje University, Gimhae, Gyungnam, Korea

Note: Supplementary data for this article are available at Cancer Research Online (http://cancerres.aacrjournals.org/).

Current address for W.-S. Chang: Allergy TF, Center for Immunology and Pathology, Korea National Institute of Health, Korea Center for Disease Control and Prevention, Seoul, Korea

Corresponding Author: Chang-Yuil Kang, Seoul National University, San 56-1, Shillim-dong, Kwanak-gu, Seoul 151-742, Korea. Phone: 82-2-880-7860; Fax: 82-2-885-1373; E-mail: cykang@snu.ac.kr

doi: 10.1158/0008-5472.CAN-13-0545

Published OnlineFirst July 18, 2013; DOI: 10.1158/0008-5472.CAN-13-0545

from Charles River Laboratories and C57BL/6 CD45.1 congenic mice were purchased from JAX. The mice were bred and maintained in the Animal Facility for Pharmaceutical Research at Seoul National University under specific pathogen-free conditions.

CT26 colon adenocarcinoma cell line, EL4 lymphoma cell line, and TC-1 lung carcinoma were obtained from the American Type Culture Collection. Human Her-2/neu–expressing transfectoma Her-2/CT26 cells were developed by transduction of CT26 using a retroviral vector system (16, 17). Cells were maintained in Dulbecco's Modified Eagle Medium or RPMI-1640 medium supplemented with 10% heat-inactivated FBS, 1% penicillin–streptomycin (G418 was supplemented for transfectoma). Cell lines were periodically authenticated by morphologic inspection and passaged for not more than 3 to 4 weeks from thawing.

Antibodies and flow cytometry

Anti-CD11b, CD27-APC, anti-Ly6G-PE/Cy7 (BioLegend), anti-F4/80, CD4 (eBioscience), CD11c (BD Biosciences), CD14, CD49b, CD8, B220, NK1.1, NKp46-PE, anti-CD3, CD19, Gr1-PerCP/Cy5.5, anti-CD122, CD45.1, Ly6C-FITC, and anti-CD45.2-PacificBlue (BioLegend) antibodies were used. IL-2–neutralizing Ab and IL-2–receptor β-blocking Ab were obtained from S4B6 and TMβ1 hybridomas, respectively, and were kind gifts from Charles D. Surh (Scripps Institute, La Jolla, California). To analyze the stained cells, FACSCalibur (BD Biosciences) instrument and FlowJo (Treestar) were used.

In vitro T-cell suppression assay

The DO11.10 cells (1×10^5/well) were stimulated with OVA protein (grade V; Sigma-Aldrich) and were cocultured with or without cytokine-induced MDSCs for 72 hours. For the final 20 to 24 hours, we added 1 μCi per well [^{3}H]-thymidine. The incorporation of the [^{3}H]-thymidine into the divided cells was detected using a liquid scintillation counter (Wallac).

ROS production, arginase 1 activity, and NO production

For ROS detection, cells were incubated in the presence of 2.5 μmol/L DCFDA ± 30 ng/mL phorbol 12-myristate 13-acetate (PMA) for 30 minutes. The fluorescence intensity of DCFDA was analyzed by flow cytometry.

Cells were incubated with 2 ng/mL IFN-γ and 100 ng/mL lipopolysaccharide (LPS) for 18 hours. To detect NO production, supernatants were collected and mixed with equal volumes of Greiss reagent (1% sulfanilamide in 5% phosphoric acid and 0.1% N-1-naphthylethylenediamine dihydrochloride in DW), after 10 minutes the absorbance at 540 nm was measured. The concentrations were determined by the standard curve of serial dilution of sodium nitrite. Arginase 1 activity was measured in cell lysates (lysed with 0.1% Triton X-100). Subsequently, 50 μL of 10 mmol/L $MnCl_2$, 50 mmol/L Tris/HCl were added and the enzyme was activated by heating for 10 minutes at 55°C. Arginine hydrolysis was conducted by incubating the lysates with 0.5 mol/L arginine (pH 9.7) at 37°C for 80 minutes. The reaction was stopped with 400 μL of acid mixture ($H_2SO_4/H_3PO_4/H_2O$ = 1/3/7). Urea production was measured at 540 nm after addition of 9% α-isonitrosopropiophenone (control absorbance subtracted from specific absorbance).

In vivo IL-2/αIL-2 Ab complex (IL-2 complex) treatment

To verify the effect of IL-2 on MDSC accumulation and function *in vivo*, we used an IL-2 complex. Mice received an intraperitoneal injection of 1.5 μg rmIL-2 plus 50 μg αIL-2 antibody. Before injection, rmIL-2 and the αIL-2 Ab were mixed and incubated at room temperature for 15 minutes.

Tumor model and isolation of tumor-infiltrating lymphocytes

C57BL/6 mice were injected subcutaneously with 2×10^5 TC-1 tumor cells. Injection of IL-2 complex began on day 1 after tumor injection. IL-2 complex treatment was administered every other day for a total of 5 or 10 times. The volume of the implanted tumor was evaluated for 19 days following the subcutaneous tumor inoculation. To separate the tumor-infiltrating lymphocytes, the tumors were collected and weighed and single-cell suspensions were prepared. The tumor was cut into small pieces and was incubated at 37°C for 0.5 hours in RPMI-1640 containing 1 mg/mL collagenase (Roche), 500 μg/mL DNase I, and 25 μg/mL hyaluronidase (Sigma).

Cell sorting

To sort CD49b$^+$ cells, splenocytes were prepared from tumor-bearing mice. To enrich the desired cell population, CD4$^+$, CD8$^+$, B220$^+$, and Ly6G$^+$ cells were depleted using microbeads (Miltenyi Biotec). CD11b$^+$Ly6C$^{neg/low}$Ly6G$^-$CD49b$^+$ cells were sorted by using FACSAria II. To sort the conventional NK cells, splenocytes were enriched by the depletion of CD4, CD8, CD19, and Ly6G$^+$ cells using microbeads. CD3$^-$CD19$^-$Gr1$^-$CD122$^+$NK1.1$^+$/NKp46$^+$ cells were sorted.

In vivo conversion assay of NK cells

To determine the conversion of NK cells *in vivo*, EL4 tumor cells were injected subcutaneously into CD45.2 mice. After 3 weeks, 2.5×10^5 CD27^{high} NK cells (CD11b^{low}CD27^{high}: CD11b^{high}CD27^{high} = 1:2) were isolated from the spleen and were transferred intravenously into CD45.1 naïve mice or mice that were inoculated subcutaneously with 1×10^5 tumor cells 7 days before the adoptive transfer. On day 14 after the transfer, CD45.2$^+$CD45.1$^-$ cells were analyzed for the expression of NK cell and MDSC markers in the spleen. For conversion assay in intraperitoneal tumor model, EL4 tumor cells were injected subcutaneously into CD45.1 congenic mice. After 3 weeks, NK1.1$^+$ cells were isolated from the spleen by FACS ARIA III and transferred intraperitoneally into naïve mice (NK1.1$^-$ –> naïve host) or mice that had been inoculated with 1×10^6 EL4 tumor cells 5 days before the adoptive transfer (NK1.1$^-$ –> tumor host), with a daily injection of IL-2 complex until sacrifice (NK1.1$^-$ –> tumor host + IL-2). On day 9 after the adoptive transfer, cells were collected from the peritoneal cavity and CD45.1$^+$CD45.2$^-$ cells were analyzed.

Published OnlineFirst July 18, 2013; DOI: 10.1158/0008-5472.CAN-13-0545

Quantitative real-time PCR

Total RNA was extracted using the TRIzol reagent and cDNA was generated with SuperScript reverse transcriptase and oligo (dT) primers (all from Invitrogen Life Technologies). The LightCycler optical system (Roche) and the SYBR Green real-time PCR Kit (Takara) were used for the analysis of gene expression. Target gene values were calculated relative to *Hprt* expression. The following primer pairs were used:

Cd122 antisense (GGAACGACCCGAGGATCAG); *Cd116* sense (AACGTGACTGACAGG AAGG); *Cd116* antisense (TGTGTGTG-CTGGCTGTTAAGG); *Cd131* sense (AAGAGCCTGCAACTCAC-TGGCAC); *Cd131* antisense (TGGGGGTTTGGCTCCACTCAT-CTT); *Cebpα* sense (CCCCAGTCAGACCAGAAAGC); *Cebpα* antisense (TGGTCCCCGTGTCCTCCTA); *Nfil3* sense (AAGGGC-CCCATCCATTCTC); *Nfil3* antisense (TTCAAACTCGCTGTC-CAAAGC); *Pu.1* sense (GCCTCAGTCACCAGGTTTCC); *Pu.1* antisense (CTCTCACCCTCCTCCTCATCTG); *Hprt* sense (AAGACTTGCTCGAGATGTCATGAA); and *Hprt* antisense (ATCCAGCAGGTCAGCAAAGAA).

Statistical analysis

Statistical analyses were conducted using Student *t* test. The results with values of $P < 0.05$ were considered to be statistically significant.

Results

Inverse relationship between the percentage of CD11b$^+$ Ly6G$^-$Ly6C$^{neg/low}$ cells and MDSCs reveals the conversion of NK-phenotype cells into MDSCs.

To explore the development of tumor-associated MDSCs, we used animal models of Her-2–expressing CT26 colon carcinoma and EL4 thymoma. When these tumor cells were subcutaneously inoculated into mice, we observed that the percentage of Ly6C$^{neg/low}$ cells (R1) among CD11b$^+$ population gradually declined in the spleen during tumor progression (Supplementary Fig. S1A and S1B). In contrast, Ly6G^{high} PMN-MDSCs (R2) and Ly6C^{high} Mo-MDSCs (R3) significantly increased in tumor-bearing mice compared with those in naïve mice. This observation led us to hypothesize that the tumor environment promotes the conversion of CD11b$^+$Ly6G$^-$Ly6C$^{neg/low}$ cells into MDSCs. To address this hypothesis, we cultured CD11b$^+$Ly6G$^-$Ly6C$^{neg/low}$ cells with cytokines that are known to be relevant to MDSC accumulation (4) and found that most of the cytokines tested induced them to become Ly6G^{high} and/or Ly6C^{high} cells, although the extent varied depending on the cytokine used (Supplementary Fig. S2A). Considering the number of live converted cells and the proportions of Ly6C^{high}/Ly6G^{high} cells after incubation, granulocyte macrophage colony-stimulating factor (GM-CSF) was the most efficient cytokine at converting Ly6C$^{neg/low}$ cells into MDSCs *in vitro* (Supplementary Fig. S2B and S2C).

Flow cytometric analysis revealed that the majority of CD11b$^+$Ly6G$^-$Ly6C$^{neg/low}$ cells expressed CD49b, but not CD14, CD11c, CD4, CD8, and B220 (Supplementary Fig. S2D). Furthermore, fluorescence-activated cell sorting (FACS)-sorted CD49b$^+$ cells (purity > 98%) obtained from tumor-bearing mice were converted into Ly6G^{high}Ly6C^{high} MDSC-like cells upon stimulation with GM-CSF (data not shown). To directly ask whether NK cells can be converted into MDSCs, we purely isolated NK1.1$^+$ and CD49b$^+$NKp46$^+$ cells from C57BL/6 and BALB/c mice, respectively, and stimulated them with GM-CSF. As depicted in Fig. 1A, GM-CSF downregulated the NK cell-markers NK1.1, CD49b, and NKp46, but instead upregulated the expression of MDSC markers Ly6C and Ly6G. Same treatment failed to induce Ly6C and Ly6G on CD4$^+$, CD8$^+$ T cells and B cells (Supplementary Fig. S3). Similarly, FACS-sorted CD49b$^+$ NKp46$^+$ cells (purity > 95%) from the bone marrow were also converted into Ly6G^{high} and Ly6C^{high} cells in the presence of GM-CSF, which was accompanied by a decrease in NK-marker expression (CD49b$^+$, 40.5%; NKp46$^+$, 14.8%). However, CD49b$^+$ NKp46$^+$ cells from the peripheral blood mononuclear cell (PBMC) did not respond to GM-CSF stimulation (data not shown).

To further investigate the observed conversion of NK cells into MDSC-like cells, we examined whether IL-2 affects this process, as this cytokine activates NK cells and potentiates NK cell-mediated antitumor activity. Notably, addition of IL-2 not only inhibited the expression of Ly6C and Ly6G triggered by GM-CSF, but also maintained the expression of NK cell-markers NK1.1, CD49b, and NKp46 (Fig. 1A).

To further investigate the role of IL-2 *in vivo*, NK1.1$^+$ cells were isolated (purity > 97%, Fig. 1B) from tumor-bearing CD45.1 mice and transferred into CD45.2 mice inoculated intraperitoneally with tumor cells 5 days before the adoptive transfer. Donor cells from the peritoneal cavity were analyzed. Up to 66% of the transferred Ly6C$^{neg/low}$NK1.1$^+$ cells were converted into Ly6C and/or Ly6G^{high} MDSCs, whereas only 20% of the cells retained NK1.1$^+$ phenotype (Fig. 1C). When the recipients were additionally given CD122-biased IL-2/IL-2–neutralizing-Ab complex (IL-2 complex; refs. 18, 19), most of the transferred cells maintained NK cell phenotype (Ly6C and/or Ly6G^{high}, 3.6%; NK1.1$^+$, 99%). In addition, there was minimal conversion of NK1.1$^+$ cells in naive recipients (Ly6C and/or Ly6G^{high}, 7%; NK1.1$^+$, 87.4%). Taken together, these results showed that NK cells can be converted into MDSC-like cells in tumor-bearing host *in vivo*, or by tumor-associated cytokines including GM-CSF *ex vivo*, and IL-2 can inhibit this conversion.

IL-2 reverses the suppressive activity of MDSCs converted from NK-phenotype cells and subverts tumor environment.

To examine whether the MDSC-like cells converted from NK cells possess immunosuppressive activity, we obtained the Ly6C^{high}Ly6G^{high} cells converted from CD49b$^+$ cells after stimulation with GM-CSF and cocultured them with DO11.10 splenocytes whose T cell receptor recognizes OVA presented by MHC II. As shown in Fig. 2B, addition of the MDSC-like cells significantly inhibited OVA-induced proliferation of DO11.10 T cells, which resembled the suppressive activity of purified PMN- and Mo-MDSCs (Fig. 2A). However, IL-2 significantly reversed the suppressive activity of the converted CD49b$^+$ cells (Fig. 2B). The converted cells also displayed ROS/NO production (Fig. 2C and D) and arginase 1 activity (Fig. 2E), by which MDSCs inhibit the immune response, but decreased level or not shown in IL-2/GM-CSF–treated or -purified CD49b$^+$ cells, indicating that the Ly6C^{high}Ly6G^{high} cells that originated from

Published OnlineFirst July 18, 2013; DOI: 10.1158/0008-5472.CAN-13-0545

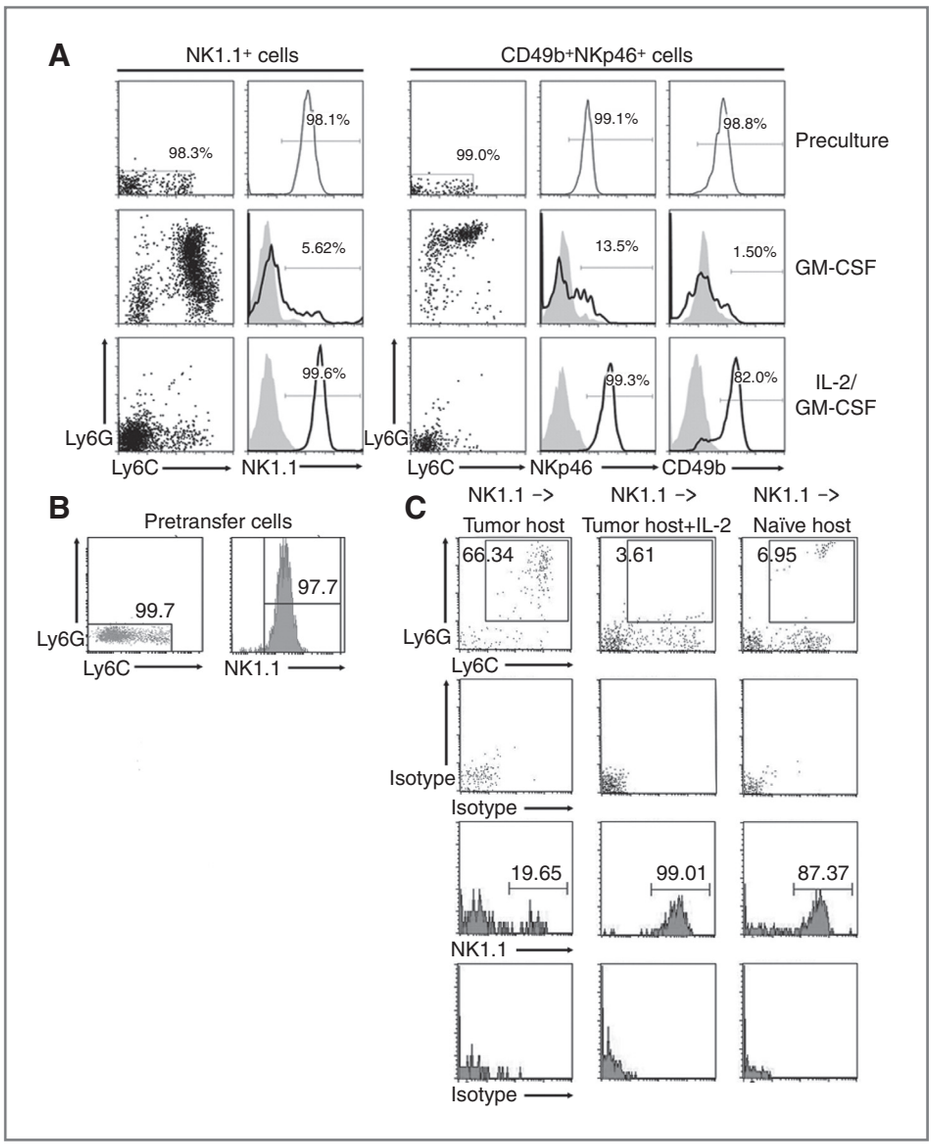

Figure 1. NK cells are converted into MDSCs. A, NK1.1$^+$ or CD49b$^+$ NKp46$^+$ cells within Ly6C$^{neg/low}$ population from spleen of tumor-bearing mice were sorted and incubated with 20 ng/mL of GM-CSF or IL-2/GM-CSF. On day 5, Ly6C/G and NK marker expression were analyzed by FACS. The numbers in the plot indicate the percentage of gated cells. The data represent 7 independent experiments. Shaded, isotype control. B and C, NK1.1$^+$ cells were isolated from CD45.1 congenic mice inoculated subcutaneously with EL4 tumor cells and were transferred intraperitoneally into CD45.2 mice. Recipient: mice injected intraperitoneally with EL4 tumor cells 5 days before the adoptive transfer (NK1.1$^-$ –> tumor host); mice injected intraperitoneally with EL4 tumor cells 5 days before the adoptive transfer and treated with IL-2 complex daily after NK1.1$^+$ cell transfer (NK1.1$^-$ –> tumor host + IL-2); and naïve mice (NK1.1$^-$ –> naïve host). C, on day 9 after the adoptive transfer, the cells were collected from the peritoneal cavity and Ly6C/G and NK1.1 expression were analyzed for CD45.1$^+$CD45.2$^-$ cells. The data were pooled from 3 mice per group. B, purity of the sorted, pretransfer NK1.1$^+$ cells. The numbers in the plot indicate the percentage of gated cells.

NK cells after GM-CSF stimulation were likely bona fide MDSCs cells with suppressive activity as well as with MDSC-signature secretion profiles.

To analyze the effect of IL-2 on MDSC populations and tumor growth, mice were treated with IL-2 complex every other day after TC-1 tumor inoculation. The tumor growth was suppressed by IL-2 treatment (Fig. 3A and B), as the proportion of MDSCs per tumor weight was reduced, although NK1.1$^+$ cells were increased among tumor-infiltrating leukocytes (Fig. 3C). However, IL-2 cessation reaccelerated the tumor growth, Ly6C^{high} MDSCs were also replenished and, importantly, NK1.1$^+$ cells were decreased in the tumor bed (Fig. 3C). In the spleen, the IL-2 counteracting effect on the frequency of MDSCs and NK cells was also prominent, although it did not have a significant effect on the cell numbers (Fig. 3D and E). This can be explained by previous studies showing that IL-2 directly or indirectly enhances the survival of granulocytes and monocytes (20–22).

CD49b$^+$ cells are prone to conversion into MDSCs in the tumor environment

To investigate whether the "MDSC-philic" cytokine-induced conversion of NK-phenotype cell into MDSCs is a property acquired in response to environmental cues or is an inherited feature, CD49b$^+$ cells were isolated from naive, 3- and 5-week tumor-bearing mice. The longer NK-phenotype cells remained in the tumor environment, the more likely they were to become Ly6C/Ly6G^{high} MDSCs following cytokine treatment. CD49b$^+$ cells from the naïve and 3-week tumor-bearing mice responded to GM-CSF; however, 50% to 60% of the cells remained CD49b$^+$ cells and the amount of CD49b$^+$ cells from the 5-week tumor-bearing mice was reduced to 19% (Fig. 4A). In addition, IL-2–mediated inhibition was less potent in CD49b$^+$ cells from the 5-week tumor-bearing mice than the 3-week tumor-bearing mice. This observation was confirmed by the increased induction of CD49b$^-$ population, which was 17% in the 5-week

Published OnlineFirst July 18, 2013; DOI: 10.1158/0008-5472.CAN-13-0545

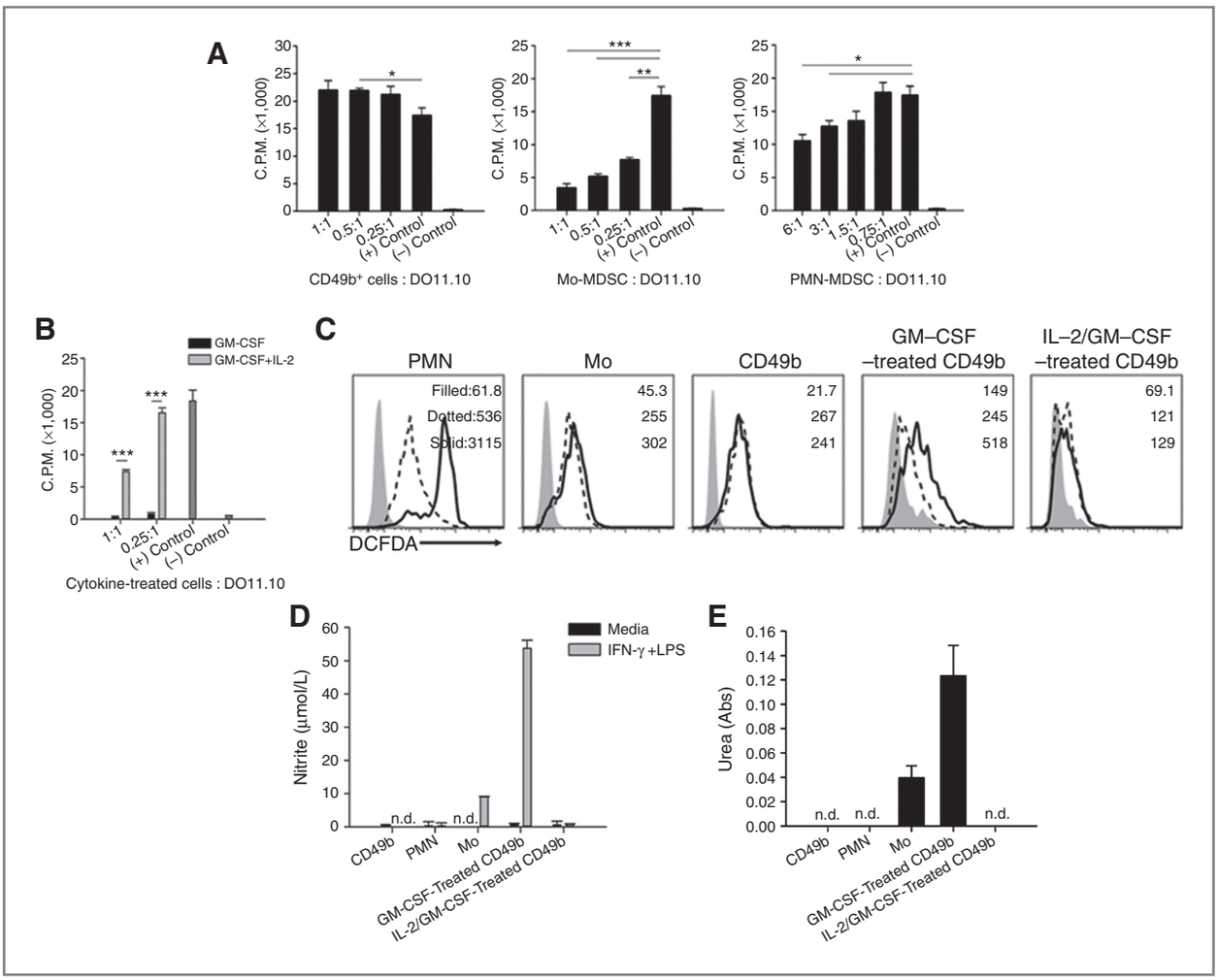

Figure 2. IL-2 reverses the suppressive activity of MDSCs converted from CD49b$^+$ cells. Purified PMN-, Mo-MDSCs, and CD49b$^+$ cells (A) or cytokine-treated CD49b$^+$ cells (B) were cocultured with DO11.10 Tg splenocytes in the presence of 250 μg/mL OVA proteins for 3 days. For the final 20 to 24 hours, we added 1 μCi per well [^{3}H]-thymidine. Incorporation of [^{3}H]-thymidine into the divided cells was detected using a liquid scintillation counter. (+) control, DO11.10 splenocytes + OVA proteins; (–) control, DO11.10 splenocytes alone. The data represent the mean ± SEM. *, $P < 0.05$; **, $P < 0.01$; ***, $P < 0.001$. C, the level of ROS in purified CD49b$^+$, PMN- and Mo-MDSC, or cytokine-treated CD49b$^+$ cells (for 4 days, 1 day rest in media before stimulation) was measured by fluorescence intensity of DCFDA labeling after PMA stimulation for 30 minutes. Filled, no PMA and no DCFDA; dotted, no PMA and DCFDA; solid, PMA and DCFDA. D and E, purified CD49b$^+$, PMN- and Mo-MDSC, or cytokine-treated CD49b$^+$ cells (for 4 days, 1 day rest in media before stimulation) were stimulated with 2 ng/mL IFN-γ and 100 ng/mL LPS for 18 hours, supernatants were collected, and nitrite concentration was measured (D). Arginase 1 activity (urea production) was measured in cell lysates (E).

tumor-bearing mice and 7% in the 3-week tumor-bearing mice in the presence of GM-CSF and IL-2 (Fig. 4A). These data indicate that NK cells may enter a conversion state that is biased toward MDSCs in the tumor environment.

The change in responsiveness to IL-2 was further shown by analyzing the related-cytokine receptors. CD49b$^+$ cells from the 5-week tumor-bearing mice preferentially expressed GM-CSF–receptor β-chain (CD131), whereas the expression of IL-2–receptor β-chain (CD122) was decreased compared with the expression in the naïve or the 3-week tumor-bearing mice. The expression of GM-CSF–receptor α-chain (CD116) did not increase significantly in the 5-week tumor-bearing mice (Fig. 4B). Although the expression of *Nfil3*, an essential regulator of NK cell development (23, 24), was decreased, the expression levels of *Cebpα* and *Pu.1*, essential transcription factors for granulocyte and monocyte development (25, 26), were significantly increased in CD49b$^+$ cells from the 5-week tumor-bearing mice compared with the naïve mice (Fig. 4B). To delineate whether the conversion was driven by these transcription factors, we analyzed the kinetics of gene expression during the cytokine stimulation. The expression of both genes was significantly downregulated, as early as 6 hours after IL-2/GM-CSF stimulation, compared with the stimulation with GM-CSF alone. The gap in the gene expression level was sustained at all the time points examined. The greatest difference was observed early for *Cebpα* expression and at a later time-point for *Pu.1* (Fig. 4C). These results suggest that the sustained expression of *Cebpα* and *Pu.1* in the presence of GM-CSF may

Published OnlineFirst July 18, 2013; DOI: 10.1158/0008-5472.CAN-13-0545

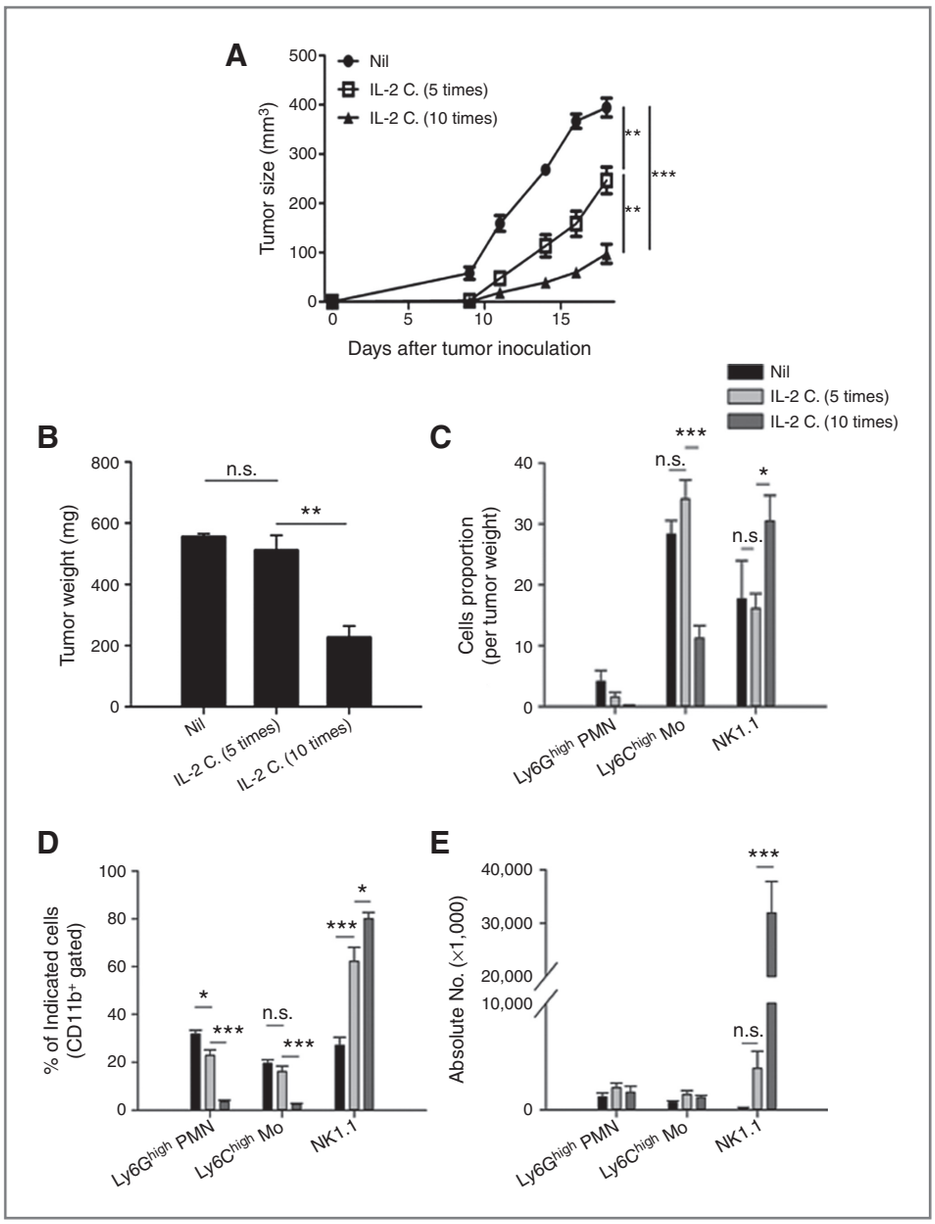

Figure 3. IL-2 subverts immunosuppressive tumor environment. A–E, C57BL/6 mice were injected subcutaneously with TC-1 tumor cells. Injection of IL-2 complex began on day 1 after tumor injection. IL-2 complex treatment was administered every other day for a total of 5 or 10 times. A, the volume of the implanted tumor was evaluated for 19 days following the subcutaneous tumor inoculation. At day 21 after tumor inoculation, tumor weight was measured (B) and the percentages and numbers of MDSCs and NK cells were analyzed in the tumor bed (C; %/tumor weight) and spleen (D and E). The data represent the mean ± SEM. *, $P < 0.05$; **, $P < 0.01$; ***, $P < 0.001$.

drive the conversion of NK-phenotype cells. However, further investigation will be needed to provide direct evidence for this hypothesis.

CD11b^{high}CD27^{high} subset of NK cells is converted into MDSCs in tumor-bearing mice

Despite prominent difference in the responsiveness to GM-CSF, we observed no significant difference in the expression of surface/transcription markers related to the lineage specification, NK cell receptors, the secretion of effector/suppressive cytokines between NK cells from naive and tumor-bearing mice (data not shown). To provide more definitive evidence for which NK cells in the tumor environment were converted into MDSCs, we further analyzed the difference in the extent of NK cell maturation based on CD11b/CD27 expression (27) between the naïve and tumor-bearing mice. The numbers of total NK cells were significantly decreased in the spleen and bone marrow of the mice inoculated with tumor cells for 3 weeks compared with naïve mice (Fig. 5A and B). Importantly, the numbers of CD11b^{high}CD27^{high} and CD11b^{high}CD27^{low} subsets among NK cells were significantly reduced in tumor-bearing mice compared with naïve mice, whereas those of the other subsets were relatively similar (Fig. 5C and D).

To elucidate whether the reduction of those NK cell populations was attributed to the observed conversion, we separated the lineage$^-$ (CD3$^-$CD19$^-$Gr1$^-$) CD122$^+$NKp46 or NK1.1$^+$ cells from tumor-bearing mice into 4 stages based on CD11b/CD27 expression level (Supplementary Fig. S4A and

Published OnlineFirst July 18, 2013; DOI: 10.1158/0008-5472.CAN-13-0545

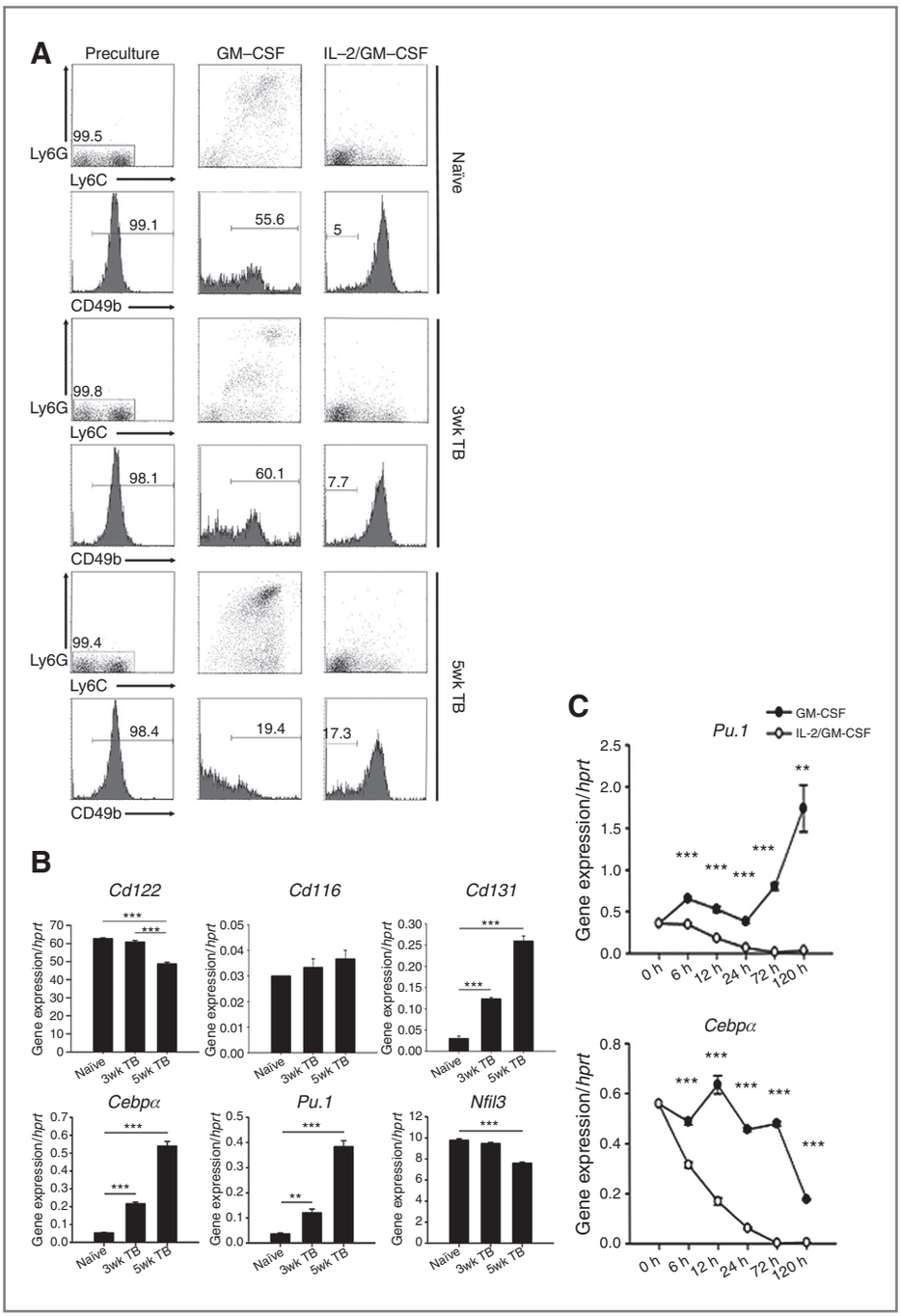

Figure 4. CD49b$^+$ cells from tumor-bearing mice are more prone to conversion into MDSCs compared with naive CD49b$^+$ cells. A, CD49b$^+$ cells isolated from naive mice and 3- and 5-week tumor-bearing mice were incubated with 20 ng/mL of the indicated cytokines. On day 5, Ly6C/G and CD49b expression were analyzed by FACS. The numbers in the plot indicate the percentage of gated cells. B, the expression of cytokine receptor genes in freshly isolated CD49b$^+$ cells from naive mice and 3- and 5-week tumor-bearing mice was measured using quantitative real-time PCR. The specific gene expression was normalized to the *Hprt* gene. The data represent the mean ± SEM. C, the kinetics of transcription factor expression during stimulation with GM-CSF or IL-2/GM-CSF. The data are representative of 3-independent experiments. **, $P < 0.01$; ***, $P < 0.001$.

S4B) and cultured them in the presence of GM-CSF. Notably, CD11b^{high}CD27^{high} NK cells obtained from tumor-bearing mice were converted into CD11b$^+$Gr1$^+$ MDSC phenotype (Fig. 6A and B), whereas their naïve counterpart and CD11b^{low}CD27^{low}, CD11b^{low}CD27^{high}, CD11b^{high}CD27^{low} NK cells from tumor-bearing mice hardly did (data not shown). Comparable purity of CD122$^+$NKp46$^+$ cells for sorting showed that the unwanted cells were present equally (0.8%–1.3%) in 4 sorted populations (Supplementary Fig. S4A), indicating that this phenomenon was not due to myeloid precursors in the tumor environment. Moreover, the GM-CSF–treated CD11b^{high}CD27^{high}NKp46$^+$ cells yielded a 3.6-fold greater number of converted cells compared with those from NKp46$^+$ cells (purity > 98.5% and 98.1%, respectively, Supplementary Fig. S5A and S5B). Furthermore, we evaluated the conversion efficiency based on the starting cell numbers. While the efficiency was only 2% in NKp46$^+$ cells, this increased to 10% in CD11b^{high}CD27^{high}NKp46$^+$ cells (Supplementary Fig. S5C), of which

Published OnlineFirst July 18, 2013; DOI: 10.1158/0008-5472.CAN-13-0545

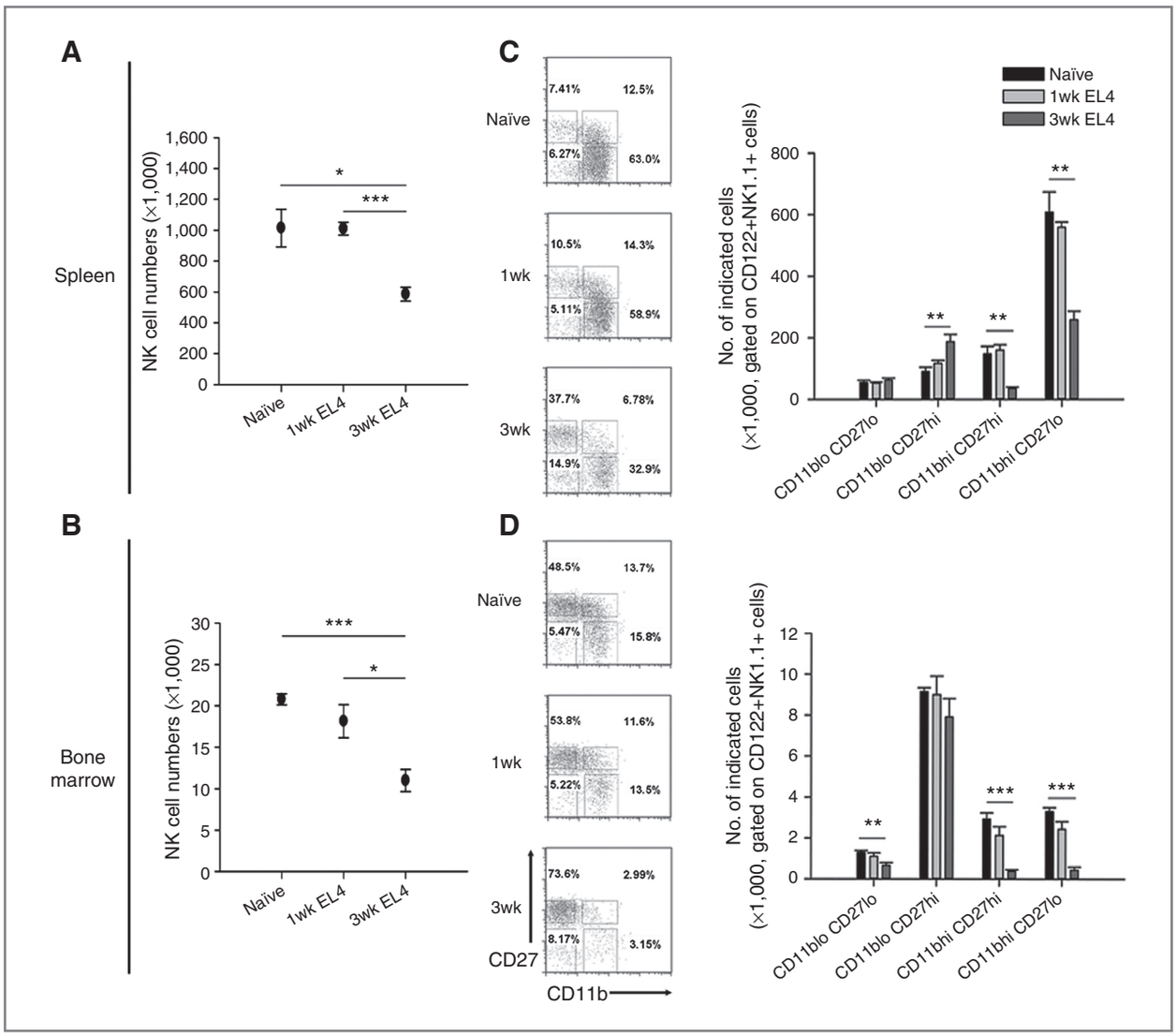

Figure 5. NK cells are decreased in tumor-bearing mice. A–D, C57BL/6 mice were injected subcutaneously with 1×10^5 EL4 tumor cells. The mice were euthanized at 1 and 3 weeks after tumor inoculation and the numbers of total NK cells (A and B) and the 4 maturation state populations (C and D) were analyzed in the spleen and bone marrow. NK cells are gated as $Lin^-CD122^+NK1.1^+$ cells ($n = 5$). The numbers in the plot indicate the percentage of gated cells. The data represent the mean ± SEM. *, $P < 0.05$; **, $P < 0.01$; ***, $P < 0.001$.

tendency was consistent with the proportion of $CD11b^{high}$ $CD27^{high}$ population included in the purified $NKp46^+$ cells (Supplementary Fig. S5A, bottom). This discrepancy in which "NK marker$^-$" cells equally included between NK populations indicates that the conversion arose from "NK marker$^+$" cells. Annexin V staining revealed that 54% of the GM-CSF–treated $CD11b^{high}CD27^{high}NKp46^+$ cells were apoptotic during the course of conversion (Supplementary Fig. S5D).

The expression of CD122, NKp46, and NK1.1 was downregulated in the presence of GM-CSF alone, whereas retained in GM-CSF/IL-2 (Fig. 6A and B). The morphology of the $CD11b^{high}CD27^{high}$ population was similar to the other populations of NK cells and the naïve $CD11b^{high}CD27^{high}$ NK cells, which exhibited a shape consistent with lymphocytes (Supplementary Fig. S4C). In contrast, ring-, segmented band-, and monocyte-shaped cells were observed after *in vitro* stimulation with GM-CSF. In the presence of GM-CSF/IL-2, the cells exhibited the morphology of activated NK cells (Fig. 6C). Another NK-activating cytokine, IL-15, also exerted an inhibitory effect on conversion upon addition of low (20 ng/mL) and high (50 ng/mL) concentrations, although low levels of $CD11b^+$ $Gr1^+$ cells (1.2%) were present after the addition of low-concentration of IL-15 (Fig. 6D).

To show this phenomenon *in vivo*, we purified $CD45.2^+CD27^{high}$ NK cells from tumor-bearing mice and transferred the cells into congenic CD45.1 mice. In tumor-bearing recipients, 12% of the transferred cells were converted into $CD11b^+Gr1^+$ MDSC phenotype (Fig. 7A and B). In addition, the expression of CD122 and NK1.1 was decreased. In contrast, the phenotype of $CD27^{high}$ NK cells was retained in naïve

Published OnlineFirst July 18, 2013; DOI: 10.1158/0008-5472.CAN-13-0545

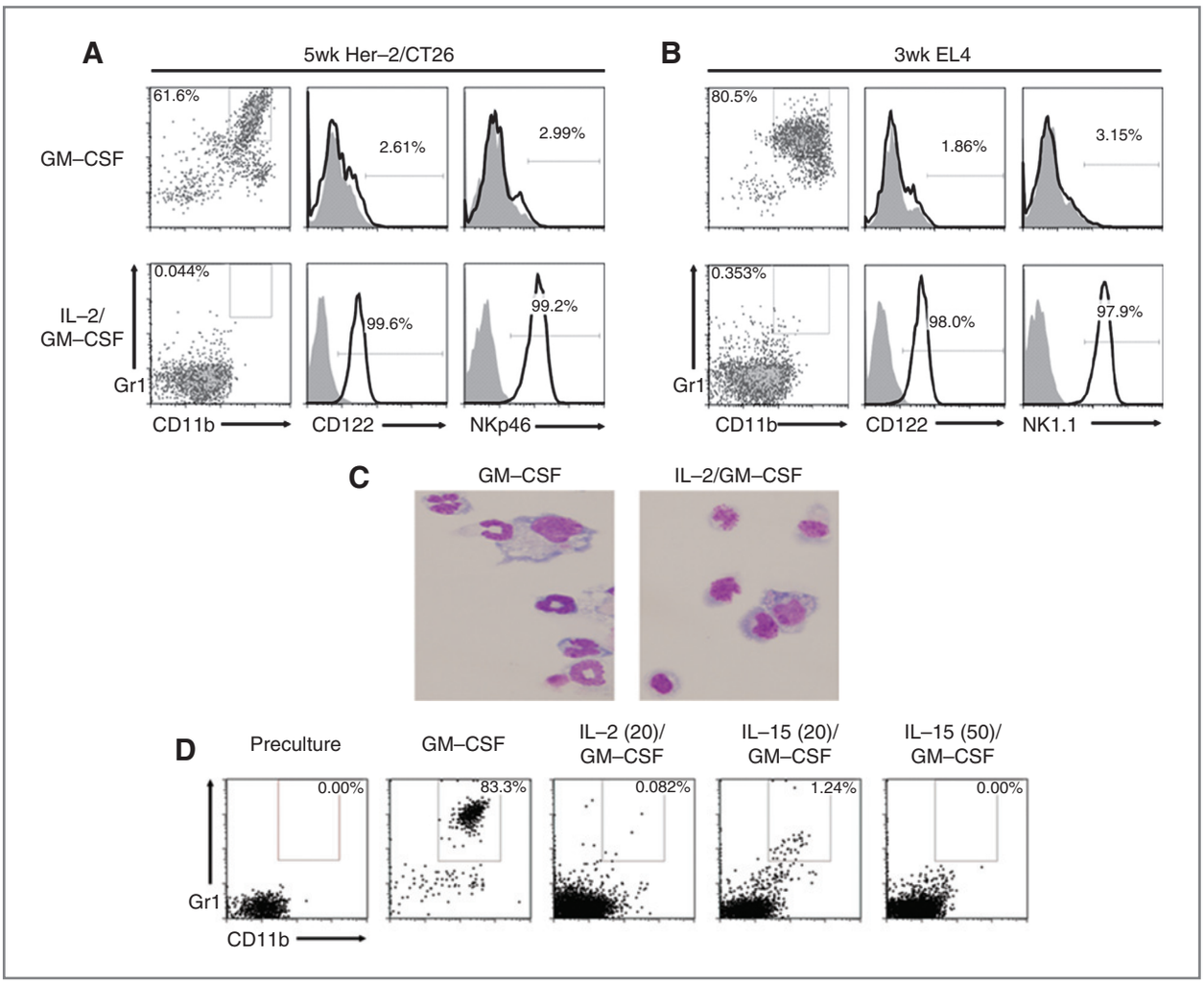

Figure 6. CD11b^{high}CD27^{high} conventional NK cells are converted into MDSCs. Among each maturation state (CD11b^{low}CD27^{low}, CD11b^{low}CD27^{high}, CD11b^{high}CD27^{high}, and CD11b^{high}CD27^{low}), Lin^{-}CD122^{+}NKp46^{+}/NK1.1^{+} CD11b^{high}CD27^{high} NK cells were sorted from tumor-bearing BALB/c (A) and C57BL/6 mice (B), respectively. Sorted cells were incubated with GM-CSF or IL-2/GM-CSF for 5 days and Gr1^{+}CD11b^{+} cell induction and CD122, NKp46, or NK1.1 expression were analyzed (the other 3 populations of NK cells hardly responded to the GM-CSF, data not shown). The data are representative of 3-independent experiments. Shaded, isotype control. C, hematoxylin and eosin staining of CD11b^{high}CD27^{high} NK cells cultured with GM-CSF or IL-2/GM-CSF for 5 days. Magnification, ×400. D, CD11b^{high}CD27^{high} NKp46^{+} cells from tumor-bearing mice were incubated with 20 ng/mL of GM-CSF ± IL-2 or IL-15. The numbers in the parenthesis indicate the concentration (ng/mL). The numbers in the plot indicate the percentage of gated cells.

recipients. Moreover, CD11b^{high}CD27^{low} NK cells and CD27^{high} NK cells from tumor-bearing and naive mice, respectively, were rarely converted into MDSCs. Furthermore, the number of CD11b^{high}CD27^{low} and CD11b^{high}CD27^{high} NK cells that arose from transferred CD27^{high} NK cells was reduced significantly in tumor-bearing recipients compared with naïve recipients (Fig. 7C–E).

However, endogenous MDSCs may cause cell death of transferred CD27^{high} NK cells, by which the matured NK cells were reduced. To investigate this, we evaluated the cell death of donor cells. The frequency of Annexin V^{+} donor cells tended to increase in the tumor-bearing host compared with the naïve host, although the difference was not statistically significant (Supplementary Fig. S6A). To examine whether MDSCs rendered donor NK cells apoptotic, we transferred MDSCs (4×10^{6}/ injection) into naive recipients 1 day before and after NK cell transfer. There was no difference in the frequency of apoptotic donor cells in the MDSC-treated naïve hosts compared with the naïve hosts (Supplementary Fig. S6A). In the same experimental setting, the donor cells were significantly more converted into MDSCs in the tumor-bearing hosts than in the naïve or MDSC-treated naïve hosts (Supplementary Fig. S6B). To more directly clarify the effect of MDSCs on NK cells during maturation, we stimulated CD45.2^{+} CD27^{high} NK cells with IL-12, -15, and -18 to mature them *in vitro* (Supplementary Fig. S6C; ref. 28). These cytokines preferentially upregulated the expression of KLRG1 and CD11b, maturation markers for NK cells, compared with the untreated NK cells. However, no differences were observed in the maturation and apoptosis of NK cells even when CD45.1^{+}MDSCs were added 3 or 6 times

Published OnlineFirst July 18, 2013; DOI: 10.1158/0008-5472.CAN-13-0545

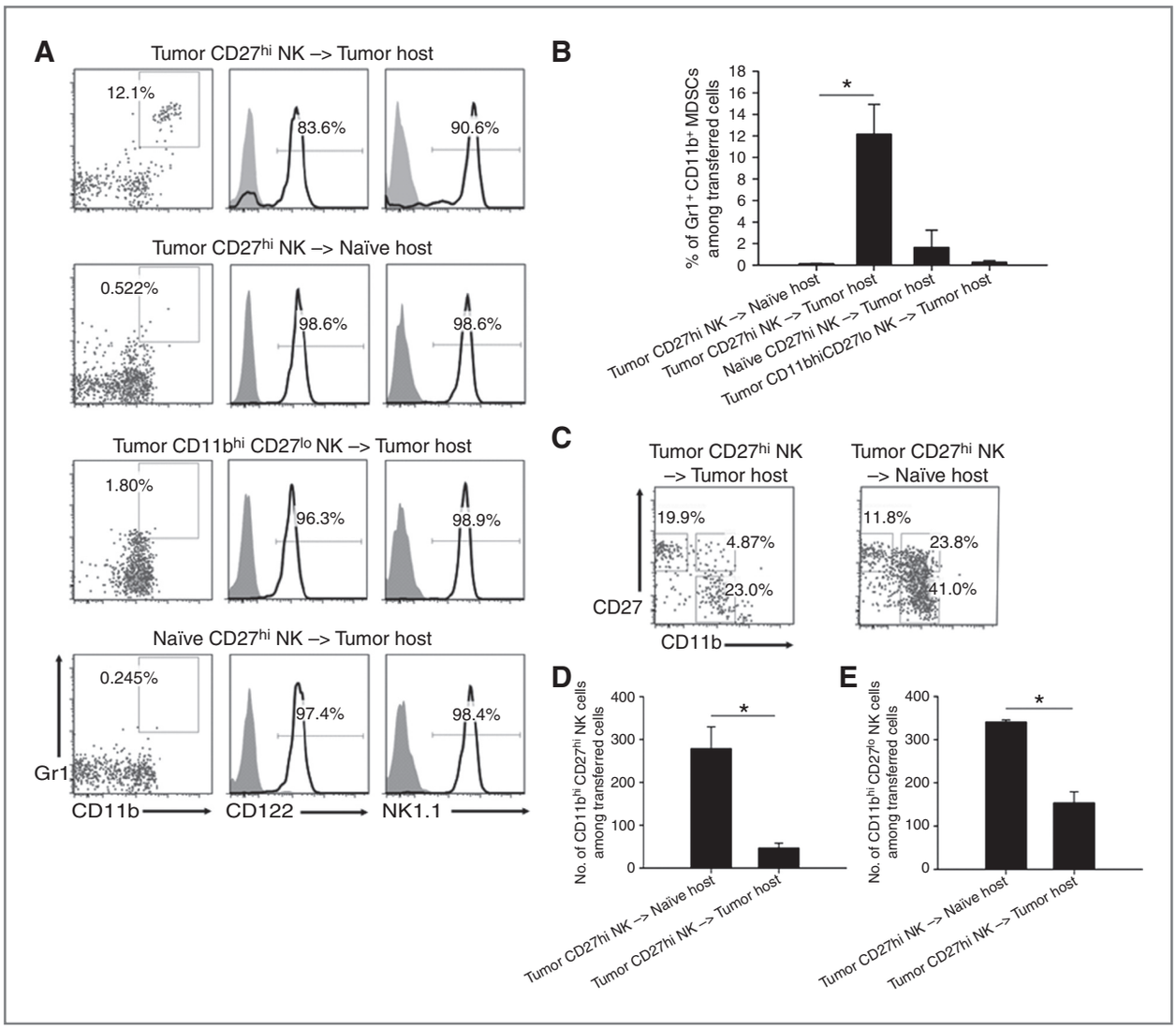

Figure 7. Conversion of CD11b^{high}CD27^{high} NK cells into MDSCs leads to CD11b^{high}CD27^{high} and CD11b^{high}CD27^{low} NK cell reduction. The conventional NK cells from the mice that were injected subcutaneously with EL4 tumor cells (CD45.2 mice) were sorted and transferred into CD45.1 tumor-bearing mice. At 2 weeks posttransfer, the recipient mice were sacrificed and were analyzed for transferred cells (CD45.2$^+$CD45.1$^-$) in the spleen. A, the percentages of Gr1$^+$CD11b$^+$ MDSCs and CD122/NK1.1 expression among the transferred cells were analyzed by FACS. B, the graph indicates the percentage of Gr1$^+$CD11b$^+$ MDSCs shown in A. C, the maturation state of NK cells was analyzed for transferred cells (CD45.2$^+$CD45.1$^-$). The graphs indicate the numbers of CD11b^{high}CD27^{high} (D) and CD11b^{high}CD27^{low} (E) NK cells derived from the transferred cells. The data represent the mean ± SEM. The data are representative of 2-independent experiments. *, $P < 0.05$ ($n = 3$). Shaded, isotype control.

compared with other conditions. These results suggested that the reduction of NK cells could be attributed to their conversion into MDSCs, and possibly cell death, in the tumor environment. However, the viability and maturation of NK cells did not seem to be influenced by endogenous MDSCs, at least in the EL4 tumor model.

Discussion

The importance of NK cells for eradicating cancer cannot be overemphasized. Several studies have reported that the tumor environment impairs the development and function of NK cells (13, 15) and even diminishes the number of NK cells in patients with chronic myelogenous leukemia (14). In this study, we determined that NK cells at a specific maturation stage were converted into immunosuppressive MDSCs, a process that was impeded by IL-2 *in vitro* and *in vivo*. The inverse relationship between the percentage of Ly6C$^{neg/low}$ cells and MDSCs provided us a clue as to which NK-phenotype cells might be converted into MDSCs. This observation led us to investigate the conversion of NKp46$^+$/NK1.1$^+$ cells and the Lin$^-$CD122$^+$ conventional NK cells. It has been reported that the expression of NKp46 is restricted to NK cells and is induced in a number of minor T-cell populations, whereas myeloid cells, such as DCs, neutrophils, and macrophages, do not express NKp46 (29), indicating that the conversion showed in this

Published OnlineFirst July 18, 2013; DOI: 10.1158/0008-5472.CAN-13-0545

study did not result from myeloid cells. Moreover, because NK cell maturation process proceeds sequentially as follows: $CD11b^{low}CD27^{neg/low}$ –> $CD11b^{low}CD27^{neg/high}$ –> $CD11b^{high}CD27^{neg/high}$ –> $CD11b^{high}CD27^{low}$ (27), the conversion of $CD11b^{high}CD27^{high}$ NK cells into MDSCs may result in the decrease of the precursors of mature $CD11b^{high}CD27^{low}$ NK cells, which led to a reduction of both populations, eventually giving rise to NK cell reduction in the tumor environment. A recent study showed that a particular population of $Ly6G^{+}Ly6C^{-}$ MDSCs impaired NK cell maturation in an IL-1β-4T1 tumor model (30). However, the viability and maturation of NK cells seemed to be minimally influenced by endogenous MDSCs *in vitro* and *in vivo*, at least in EL4 tumor model, whereas $CD27^{high}$ NK cells were converting into MDSCs (Supplementary Fig. S6).

Adoptively transferred NK cells lost NK markers and converted into MDSCs probably by tumor-derived GM-CSF, assumed by *in vitro* conversion assay shown in this study. Nevertheless, the conversion could be regulated by various cytokines released by tumor. We are supposed to clarify this by tumor cell knockdown experiments using shRNA or neutralization of cytokines in future studies.

Because the exact roles of CD27 in NK cell biology have not been fully investigated, it aroused our curiosity whether CD27–CD27 ligand signaling influenced NK cells or MDSCs. However, upon CD27-mediated signaling by the addition of recombinant ligands *in vitro*, no remarkable effect was found other than increased apoptosis during the conversion of NK cells into MDSCs (data not shown), although the ligands may play other roles *in vivo*.

We showed that the conversion of $Lin^{-}CD122^{+}$ conventional NK cells was prominent in only $CD11b^{high}CD27^{high}$ populations (Fig. 6). Four sorted populations of NK cells showed comparable purity for $CD122^{+}NKp46^{+}$ cells (Supplementary Fig. S4A), which indicates that the unwanted cells are present equally. Moreover, our morphologic analysis showed that all 4 populations of NK cells isolated from tumor-bearing mice had no difference (Supplementary Fig. S4C). Nevertheless, NK cells in the other maturation states were not converted, indicating that this phenomenon was not because of the myeloid-biased differentiation by the tumor environment, rather NK cells in a specific maturation state were converted into MDSCs.

Several studies have endeavored to explain the development, function, migration, and fate of MDSCs (31–33). A recently published study has determined that the myeloid precursors of MDSCs that reside in the spleen are relocated to tumors (34, 35). Moreover, novel transdifferentiation pathway from monocytic-to-granulocytic MDSCs driven by epigenetic regulation in the tumor environment, which is beside the classical divergent development of monocytes and granulocytes, has been revealed (33). From a different perspective, we suggest that NK-phenotype cells could be additional precursors of MDSCs. Accordingly, the precise contribution of NK cells to MDSC expansion must be examined; however, the depletion of NK cells by antibodies did not significantly influence the accumulation of MDSCs in the tumor-bearing mice (data not shown). Apart from the question of contribution, the observation that the effector NK cells were converted into suppressor cells indicated the aggravation of the immunosuppressive environment in the tumor-bearing mice, which may also apply to patients with cancer (14).

We have attempted to identify the conversion of NK cells into MDSCs in a human system. Several studies have shown that MDSCs can be produced from whole PBMCs and monocytes (36–39). However, $CD56^{+}$ cells purified from the PBMCs of patients with cancer were not converted into MDSCs (data not shown). These observations are consistent with the results from PBMC data in the mouse system, although the reason for this remains unclear. This indicates that the conversion of NK cells may depend on their anatomical location. Because in mice, NK cells from the spleen and bone marrow and not the PBMCs were converted into MDSCs, the corresponding organs in humans should be investigated. Furthermore, the types and stages of cancer confer complexity on the environments in which NK cells are influenced by various factors, which may cause confusion when predicting the conversion of NK cells into MDSCs in the human system. Therefore, more detailed and extensive investigations of human specimens classified by the type/stage of cancer and the organs from which NK cells are isolated will be required for future studies.

NK cells are thought to differentiate from common lymphoid progenitors (CLP; refs. 10, 40). However, a number of studies have debated the origin of NK cells and have shown that the cells can be derived from myeloid progenitors (41–43). It has also been reported that CLPs under certain conditions and the earliest progenitors in the thymus have the potential for myeloid development (44, 45). Whether myeloid-derived NK cells exist in the periphery and whether these cells are essential for the conversion shown in this study, are intriguing issues. Even if this were the case, myeloid-derived NK cells are only a fraction of the entire NK cell population because not all of $NK1.1^{+}$ and $CD49b^{+}NKp46^{+}$ cells were converted into MDSCs, between those only $CD11b^{high}CD27^{high}$ NK cells were converted.

The levels of *Cebpα* and *Pu.1*, essential transcription factors for the development of granulocytes and monocytes (25, 26), were increased in $CD49b^{+}$ cells from the tumor-bearing mice and may constitute a marker for NK cells that are converting into MDSCs. This idea was supported by the results of the kinetic study of the transcription factors; the relative expression levels of *Cebpα* and *Pu.1* were higher in GM-CSF–treated $CD49b^{+}$ cells compared with GM-CSF/IL-2–treated cells. Several studies have reported that the ectopic expression of *Cebpα* and *Pu.1* activates transdifferentiation (46, 47) and that these transcription factors synergistically program distinct responses to NF-κB activation (47), also can be induced by GM-CSF. Conversely, in the presence of IL-2, it is conceivable that STAT5 is phosphorylated and binds to target genes. We also identified the activation of STAT5 in NK cells in the presence of IL-2 by flow cytometric analysis (data not shown). It is assumed that IL-2–induced STAT5 then binds to the promoter of *Cebpα*/*Pu.1* in competition with STAT3, thereby inhibiting transcriptional and/or epigenetical regulation by STAT3 as shown by the opposing STAT3–STAT5

Published OnlineFirst July 18, 2013; DOI: 10.1158/0008-5472.CAN-13-0545

regulation of IL-17 expression in T_H17 cells (48). The exact molecular mechanisms that regulate the conversion of these cells into MDSCs need to be investigated further.

IL-2 has been used as an immunotherapy for patients with metastatic melanoma and metastatic-renal cell carcinoma because of its strong stimulatory effect on $CD8^+$ T cells and NK cells (49, 50). We showed that IL-2 prevented NK cells from converting into MDSCs *in vitro* and *in vivo*. However, no significant inhibitory effect on the number of MDSCs was observed in the spleen of IL-2 complex-treated tumor-bearing mice. A previous study reported that the cytokines produced from IL-2–activated NK cells prolongs the survival of granulocytes and monocytes (22) and IL-2 complex strongly activates NK cells (18). In this case, the effect on MDSC numbers in IL-2 complex-treated mice could be underestimated because of the increase in granulocytes/monocytes, which share surface markers, such as Ly6C, Ly6G, CD11b, with PMN- and Mo-MDSCs.

Collectively, the data in this study suggest that NK cell reduction resulted from the conversion of NK cells into MDSCs in the middle of the maturation stage, before $CD11b^{high}$ $CD27^{high}$ NK cells give rise to the mature $CD11b^{high}CD27^{low}$ phenotype in the tumor environment. It could be a missing part of mechanisms by which results in NK cell reduction in tumor immunosuppressive environment, suggesting a novel tumor evasion mechanism. It is also noteworthy that our data suggested the possibility of conversion between lymphoid (NK cells) and myeloid cells (MDSCs), which are derived from distinct progenitor cells.

Disclosure of Potential Conflicts of Interest

No potential conflicts of interest were disclosed.

Authors' Contributions

Conception and design: Y.-J. Park, W.-S. Chang, C.-Y. Kang
Development of methodology: Y.-J. Park, W.-S. Chang
Acquisition of data (provided animals, acquired and managed patients, provided facilities, etc.): Y.-J. Park, J.-M Lee, J.-O. Kim
Analysis and interpretation of data (e.g., statistical analysis, biostatistics, computational analysis): Y.-J. Park, B. Song, Y.-S. Kim, Y.-J. Kim
Writing, review, and/or revision of the manuscript: Y.-J. Park, J.-M Lee, Y.-J. Kim, C.-Y. Kang
Administrative, technical, or material support (i.e., reporting or organizing data, constructing databases): B. Song, E.-K. Kim, G.-E. Lee
Study supervision: C.-Y. Kang

Grant Support

This study was supported by a grant from the NRL (No. R0A-2008-000-20113-0), the WCU (No. R31-2008-000-10103-0) of the National Research Foundation of Korea (NRF), the Public Welfare & Safety Research Program (20110020963), and the National R&D Program for Cancer Control, Ministry of Health and Welfare (No. 0720500). We appreciate Dr. Charles D. Surh (Scripps Institute) and Dr. Shimon Sakaguchi (Kyoto University) for providing the TMβ1, S4B6, and PC61 hybridomas.

The costs of publication of this article were defrayed in part by the payment of page charges. This article must therefore be hereby marked *advertisement* in accordance with 18 U.S.C. Section 1734 solely to indicate this fact.

Received February 22, 2013; revised June 25, 2013; accepted June 30, 2013; published OnlineFirst July 18, 2013.

References

1. Flavell RA, Sanjabi S, Wrzesinski SH, Licona-Limon P. The polarization of immune cells in the tumour environment by TGFbeta. Nat Rev Immunol 2010;10:554–67.
2. Whiteside TL. The tumor microenvironment and its role in promoting tumor growth. Oncogene 2008;27:5904–12.
3. Zitvogel L, Tesniere A, Kroemer G. Cancer despite immunosurveillance: immunoselection and immunosubversion. Nat Rev Immunol 2006;6:715–27.
4. Gabrilovich DI, Nagaraj S. Myeloid-derived suppressor cells as regulators of the immune system. Nat Rev Immunol 2009;9:162–74.
5. Corzo CA, Condamine T, Lu L, Cotter MJ, Youn JI, Cheng P, et al. HIF-1alpha regulates function and differentiation of myeloid-derived suppressor cells in the tumor microenvironment. J Exp Med 2010;207:2439–53.
6. Ostrand-Rosenberg S, Sinha P. Myeloid-derived suppressor cells: linking inflammation and cancer. J Immunol 2009;182:4499–506.
7. Condamine T, Gabrilovich DI. Molecular mechanisms regulating myeloid-derived suppressor cell differentiation and function. Trends Immunol 2011;32:19–25.
8. Marigo I, Bosio E, Solito S, Mesa C, Fernandez A, Dolcetti L, et al. Tumor-induced tolerance and immune suppression depend on the C/EBPbeta transcription factor. Immunity 2010;32:790–802.
9. Sonda N, Chioda M, Zilio S, Simonato F, Bronte V. Transcription factors in myeloid-derived suppressor cell recruitment and function. Curr Opin Immunol 2011;23:279–85.
10. Vivier E, Raulet DH, Moretta A, Caligiuri MA, Zitvogel L, Lanier LL, et al. Innate or adaptive immunity? The example of natural killer cells. Science 2011;331:44–9.
11. Cerwenka A, Lanier LL. Natural killer cells, viruses and cancer. Nat Rev Immunol 2001;1:41–9.
12. Vivier E, Ugolini S, Blaise D, Chabannon C, Brossay L. Targeting natural killer cells and natural killer T cells in cancer. Nat Rev Immunol 2012;12:239–52.
13. Liu C, Yu S, Kappes J, Wang J, Grizzle WE, Zinn KR, et al. Expansion of spleen myeloid suppressor cells represses NK cell cytotoxicity in tumor-bearing host. Blood 2007;109:4336–42.
14. Pierson BA, Miller JS. CD56+bright and CD56+dim natural killer cells in patients with chronic myelogenous leukemia progressively decrease in number, respond less to stimuli that recruit clonogenic natural killer cells, and exhibit decreased proliferation on a per cell basis. Blood 1996;88:2279–87.
15. Sibbitt WL Jr, Bankhurst AD, Jumonville AJ, Saiki JH, Saiers JH, Doberneck RC. Defects in natural killer cell activity and interferon response in human lung carcinoma and malignant melanoma. Cancer Res 1984;44:852–6.
16. Chang SY, Lee KC, Ko SY, Ko HJ, Kang CY. Enhanced efficacy of DNA vaccination against Her-2/neu tumor antigen by genetic adjuvants. Int J Cancer 2004;111:86–95.
17. Chung Y, Kim BS, Kim YJ, Ko HJ, Ko SY, Kim DH, et al. CD1d-restricted T cells license B cells to generate long-lasting cytotoxic antitumor immunity *in vivo*. Cancer Res 2006;66:6843–50.
18. Boyman O, Kovar M, Rubinstein MP, Surh CD, Sprent J. Selective stimulation of T cell subsets with antibody-cytokine immune complexes. Science 2006;311:1924–7.
19. Letourneau S, van Leeuwen EM, Krieg C, Martin C, Pantaleo G, Sprent J, et al. IL-2/anti-IL-2 antibody complexes show strong biological activity by avoiding interaction with IL-2 receptor alpha subunit CD25. Proc Natl Acad Sci U S A 2010;107:2171–6.
20. Akgul C, Moulding DA, Edwards SW. Molecular control of neutrophil apoptosis. FEBS Lett 2001;487:318–22.
21. Heidenreich S. Monocyte CD14: a multifunctional receptor engaged in apoptosis from both sides. J Leukoc Biol 1999;65:737–43.
22. Bhatnagar N, Hong HS, Krishnaswamy JK, Haghikia A, Behrens GM, Schmidt RE, et al. Cytokine-activated NK cells inhibit PMN apoptosis and preserve their functional capacity. Blood 2010;116:1308–16.

23. Di Santo JP. Natural killer cell developmental pathways: a question of balance. Annu Rev Immunol 2006;24:257–86.
24. Ramirez K, Kee BL. Multiple hats for natural killers. Curr Opin Immunol 2010;22:193–8.
25. Ceredig R, Rolink AG, Brown G. Models of haematopoiesis: seeing the wood for the trees. Nat Rev Immunol 2009;9:293–300.
26. Iwasaki H, Akashi K. Myeloid lineage commitment from the hematopoietic stem cell. Immunity 2007;26:726–40.
27. Chiossone L, Chaix J, Fuseri N, Roth C, Vivier E, Walzer T. Maturation of mouse NK cells is a 4-stage developmental program. Blood 2009; 113:5488–96.
28. Ni J, Miller M, Stojanovic A, Garbi N, Cerwenka A. Sustained effector function of IL-12/15/18-preactivated NK cells against established tumors. J Exp Med 2012;209:2351–65.
29. Narni-Mancinelli E, Chaix J, Fenis A, Kerdiles YM, Yessaad N, Reynders A, et al. Fate mapping analysis of lymphoid cells expressing the NKp46 cell surface receptor. Proc Natl Acad Sci U S A 2011;108: 18324–9.
30. Elkabets M, Ribeiro VS, Dinarello CA, Ostrand-Rosenberg S, Di Santo JP, Apte RN, et al. IL-1beta regulates a novel myeloid-derived suppressor cell subset that impairs NK cell development and function. Eur J Immunol 2010;40:3347–57.
31. Cheng P, Corzo CA, Luetteke N, Yu B, Nagaraj S, Bui MM, et al. Inhibition of dendritic cell differentiation and accumulation of myeloid-derived suppressor cells in cancer is regulated by S100A9 protein. J Exp Med 2008;205:2235–49.
32. Ma G, Pan PY, Eisenstein S, Divino CM, Lowell CA, Takai T, et al. Paired immunoglobin-like receptor-B regulates the suppressive function and fate of myeloid-derived suppressor cells. Immunity 2011;34:385–95.
33. Youn JI, Kumar V, Collazo M, Nefedova Y, Condamine T, Cheng P, et al. Epigenetic silencing of retinoblastoma gene regulates pathologic differentiation of myeloid cells in cancer. Nat Immunol 2013;14: 211–20.
34. Cortez-Retamozo V, Etzrodt M, Newton A, Rauch PJ, Chudnovskiy A, Berger C, et al. Origins of tumor-associated macrophages and neutrophils. Proc Natl Acad Sci U S A 2012;109:2491–6.
35. Bayne LJ, Beatty GL, Jhala N, Clark CE, Rhim AD, Stanger BZ, et al. Tumor-derived granulocyte-macrophage colony-stimulating factor regulates myeloid inflammation and T cell immunity in pancreatic cancer. Cancer Cell 2012;21:822–35.
36. Lechner MG, Liebertz DJ, Epstein AL. Characterization of cytokine-induced myeloid-derived suppressor cells from normal human peripheral blood mononuclear cells. J Immunol 2010;185:2273–84.
37. Lechner MG, Megiel C, Russell SM, Bingham B, Arger N, Woo T, et al. Functional characterization of human Cd33+ and Cd11b+ myeloid-derived suppressor cell subsets induced from peripheral blood mononuclear cells cocultured with a diverse set of human tumor cell lines. J Transl Med 2011;9:90.
38. Obermajer N, Kalinski P. Generation of myeloid-derived suppressor cells using prostaglandin E2. Transplant Res 2012;1:15.
39. Obermajer N, Muthuswamy R, Lesnock J, Edwards RP, Kalinski P. Positive feedback between PGE2 and COX2 redirects the differentiation of human dendritic cells toward stable myeloid-derived suppressor cells. Blood 2011;118:5498–505.
40. Kondo M, Weissman IL, Akashi K. Identification of clonogenic common lymphoid progenitors in mouse bone marrow. Cell 1997; 91:661–72.
41. Grzywacz B, Kataria N, Blazar BR, Miller JS, Verneris MR. Natural killer-cell differentiation by myeloid progenitors. Blood 2011;117: 3548–58.
42. Marquez C, Trigueros C, Franco JM, Ramiro AR, Carrasco YR, López-Botet M, et al. Identification of a common developmental pathway for thymic natural killer cells and dendritic cells. Blood 1998;91:2760–71.
43. Perez SA, Sotiropoulou PA, Gkika DG, Mahaira LG, Niarchos DK, Gritzapis AD, et al. A novel myeloid-like NK cell progenitor in human umbilical cord blood. Blood 2003;101:3444–50.
44. Kondo M, Scherer DC, Miyamoto T, King AG, Akashi K, Sugamura K, et al. Cell-fate conversion of lymphoid-committed progenitors by instructive actions of cytokines. Nature 2000;407:383–6.
45. Luc S, Luis TC, Boukarabila H, Macaulay IC, Buza-Vidas N, Bouriez-Jones T, et al. The earliest thymic T cell progenitors sustain B cell and myeloid lineage potential. Nat Immunol 2012;13:412–9.
46. Ghisletti S, Barozzi I, Mietton F, Polletti S, De Santa F, Venturini E, et al. Identification and characterization of enhancers controlling the inflammatory gene expression program in macrophages. Immunity 2010; 32:317–28.
47. Jin F, Li Y, Ren B, Natarajan R. PU.1 and C/EBP(alpha) synergistically program distinct response to NF-kappaB activation through establishing monocyte specific enhancers. Proc Natl Acad Sci U S A 2011; 108:5290–5.
48. Yang XP, Ghoreschi K, Steward-Tharp SM, Rodriguez-Canales J, Zhu J, Grainger JR, et al. Opposing regulation of the locus encoding IL-17 through direct, reciprocal actions of STAT3 and STAT5. Nat Immunol 2011;12:247–54.
49. Klapper JA, Downey SG, Smith FO, Yang JC, Hughes MS, Kammula US, et al. High-dose interleukin-2 for the treatment of metastatic renal cell carcinoma: a retrospective analysis of response and survival in patients treated in the surgery branch at the National Cancer Institute between 1986 and 2006. Cancer 2008;113:293–301.
50. Rosenberg SA, Yang JC, Topalian SL, Schwartzentruber DJ, Weber JS, Parkinson DR, et al. Treatment of 283 consecutive patients with metastatic melanoma or renal cell cancer using high-dose bolus interleukin 2. JAMA 1994;271:907–13.